Abnormal thalamocortical network dynamics in migraine

Yiheng Tu, PhD,* Zening Fu, PhD,* Fang Zeng, MD, PhD,* Nasim Maleki, PhD, Lei Lan, MD, PhD, Zhengjie Li, MD, PhD, Joel Park, BA, Georgia Wilson, BA, Yujie Gao, MD, PhD, Mailan Liu, MD, PhD, Vince Calhoun, PhD, Fanrong Liang, MD, MS and Jian Kong, MD, MS, MPH

Neurology® 2019;92:e2706-e2716. doi:10.1212/WNL.0000000000007607

Correspondence
Dr. Kong
kongj@
nmr.mgh.harvard.edu
or Dr. Liang
acuresearch@126.com

Abstract

Objective
To investigate the dynamic functional connectivity of thalamocortical networks in interictal migraine patients and whether clinical features are associated with abnormal connectivity.

Methods
We investigated dynamic functional network connectivity (dFNC) of the migraine brain in 89 interictal migraine patients and 70 healthy controls. We focused on the temporal properties of thalamocortical connectivity using sliding window cross-correlation, clustering state analysis, and graph-theory methods. Relationships between clinical symptoms and abnormal dFNC were evaluated using a multivariate linear regression model.

Results
Five dFNC brain states were identified to characterize and compare dynamic functional connectivity patterns. We demonstrated that migraineurs spent more time in a strongly interconnected between-network state, but they spent less time in a sparsely connected state. Interestingly, we found that abnormal posterior thalamus (pulvinar nucleus) dFNC with the visual cortex and the precuneus were significantly correlated with headache frequency of migraine. Further topologic measures revealed that migraineurs had significantly lower efficiency of information transfer in both global and local dFNC.

Conclusion
Our results demonstrated a transient pathologic state with atypical thalamocortical connectivity in migraineurs and extended current findings regarding abnormal thalamocortical networks and dysrhythmia in migraine.

Glossary

AUC = area under the curve; **AUD** = auditory domain; **CC** = cognitive control domain; **dFNC** = dynamic functional network connectivity; **DM** = default mode domain; **FC** = functional connectivity; **FDR** = false discovery rate; **GICA** = group independent component analysis; **HC** = healthy controls; **ICHD** = International Classification of Headache Disorders; **ICN** = intrinsic component network; **IRB** = institutional review board; **MIG** = migraine without aura patients; **MNI** = Montreal Neurologic Institute; **rsFC** = resting-state functional connectivity; **SAS** = self-rating anxiety scale; **SC** = subcortical domain; **SDS** = self-rating depression scale; **SM** = sensorimotor domain; **TCD** = thalamocortical dysrhythmia; **TE** = echo time; **TR** = repetition time; **VS** = visual domain.

With its broad connectivity and prominent role in state changes, cortical gain modulation, and allodynia, the thalamus may be a key node of thalamocortical dysfunction in migraine. Neuroimaging studies have revealed that thalamocortical dysrhythmia[1] and abnormal low-frequency oscillations in thalamocortical networks[2] are associated with clinical migraine symptoms and underlie important processes involved in multisensory integration. However, this has not been investigated using functional connectivity (FC), which could provide fine spatial resolution for studying functional interactions.

Conventional resting-state FC (rsFC) studies assume that functional interactions remain constant throughout the entire resting-state scan. In reality, individuals engage in different mental states that cannot be experimentally controlled.[3] Recent studies have shown that rsFC can vary considerably in different temporal scales.[4–6] Time-varying characteristics may represent spontaneous alterations in the underlying networks and thus may reveal neural mechanisms that cannot be discovered through static rsFC alone.[5–8]

In this study, we examined dynamic rsFC in 89 migraine without aura patients (MIG) and 70 healthy controls (HC). We hypothesized that migraine would be associated with dynamic connectivity abnormalities of the thalamocortical networks, which would be correlated with clinical characteristics. We investigated the transient changes of rsFC and the dynamics of the global and local efficiency of information transfer in migraineurs.

Methods

Standard protocol approvals, registrations, and patient consents

This study was done as a baseline session of a registered clinical trial listed on clinicaltrials.gov (NCT01152632, June 27, 2010). The institutional review board (IRB) of Chengdu University of Traditional Chinese Medicine approved the study, and all experiments were performed in accordance with the guidelines set forth by the IRB for ethics and protection of human participants. All participants gave their written informed consent and were compensated for their participation.

Participants

The study included 100 MIG and 70 demographically matched HC. Recruitment started in June 2011 and ended in November 2013. Migraine patients were diagnosed by 3 neurologists based on the International Classification of Headache Disorders (ICHD), 2nd Edition, migraine without aura criteria,[9] which is compatible with ICHD-III. All participants were recruited from the general population via advertisements, and patients were required to stop taking any prophylactic headache medicine during the last month of the study. In order to minimize the effects of a prior headache or an impending headache, all migraine patients in this study were migraine-free for at least 72 hours at the time of the MRI scan. Details of the inclusion criteria can be found in appendix e-1 (doi.org/10.5061/dryad.p1n53q4).

Data acquisition

All functional MRI data were acquired on a 3.0T magnetic resonance scanner (Siemens 3.0T TIM Trio, Munich, Germany) with an 8-channel phase-array head coil at the West China Hospital MRI center. Participants were asked to stay awake and to keep their heads still during the scan, with their eyes closed and ears plugged. Prior to the functional run, a high-resolution structural image for each participant was acquired using a 3D T1-weighted MRI pulse sequence (magnetization-prepared rapid gradient echo) with a voxel size of 1 mm^3 employing an axial fast spoiled gradient recalled sequence (repetition time [TR] 1,900 ms; echo time [TE] 2.26 ms; data matrix 256 × 256; field of view 256 × 256 mm^2). The blood oxygenation level–dependent resting-state functional images were obtained with echo-planar imaging (30 contiguous slices with a slice thickness of 5 mm; TR 2,000 ms; TE 30 ms; flip angle 90°; field of view 240 × 240 mm^2; data matrix 64× 64; total volumes 180).

fMRI data preprocessing and head motion analysis

We preprocessed and analyzed the fMRI data using SPM12 (Wellcome Trust Centre for Neuroimaging, London, UK). We discarded the first 10 volumes to allow for signal equilibration. Images were corrected for slice-timing and head motion. The resulting images were normalized to the Montreal Neurologic Institute (MNI) space[10] and spatially smoothed using a Gaussian kernel of 5 mm full width at half maximum.

To minimize the effect of head motion on the estimation of FC, we followed the strategy suggested by a recent benchmark study[11] of combining the 6 motion estimates and 2 physiologic time series (CSF and the white matter signals) with global signal regression. We also compared the maximal framewise displacement value of head motion between MIG and HC. Detailed results are available in appendix e-2 (doi.org/10.5061/dryad.p1n53q4).

Behavioral assessments

We used migraine frequency (number of attacks, separated by pain-free intervals of at least 48 hours, per month) and intensity (0–10 scores; 0: no pain, 10: worst pain imaginable) during the past month as clinical measures for MIG.[12] Patients recorded these values in a migraine diary. Anxiety and depression levels were measured using the self-rating anxiety scale (SAS)[13] and the self-rating depression scale (SDS),[14] respectively.

Dynamic functional network connectivity (dFNC) state analysis

The framework of characterizing dynamic rsFC to detect atypical functional dynamics in migraine is shown in figure 1,

and the technical details pertaining to each step are described in the following sections. There were 4 major steps in this framework. In step 1, we first conducted a group independent component analysis (GICA)[15] to decompose whole brain resting-state fMRI data into multiple independent components (figure 1.1). Following GICA, we selected intrinsic component networks (ICNs) from the independent components according to their spatial activation maps. In step 2, we calculated dFNC among ICNs using a sliding window approach with graphic LASSO (see below; figure 1.2). In step 3, we conducted a k-means-based hard clustering on the dFNC estimates to identify distinct FC states (dFNC states) and the frequency of their occurrence, which together allowed us to construct a profile of the brain connectivity dynamics during a given period for each participant (figure 1.3). The profile derived for one participant is shown in figure 1.3C. This profile captures changes in the dFNC state for each participant during a 6-minute scan. Next, we performed an additional analysis to determine the highly reoccurring dFNC states in each group. In step 4, we applied graph theory measures on different dFNC states to demonstrate that the efficiency of information transfer in dynamic brain networks is variable.

Figure 1 Analysis flowchart to study dynamic functional network connectivity (dFNC) in migraine patients
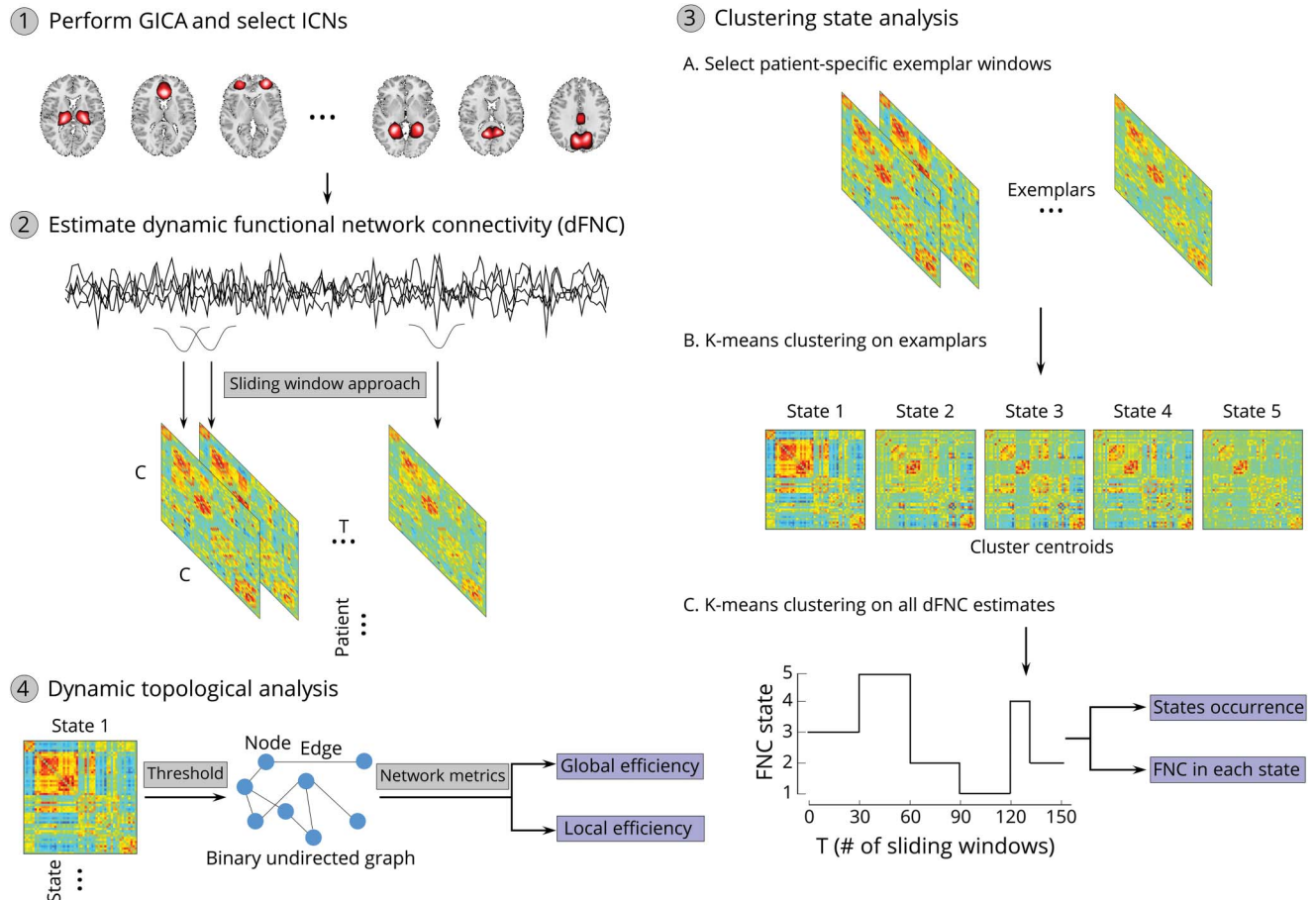
Four major steps were included: (1) perform group independent component analysis (GICA) and select intrinsic connectivity networks (ICNs); (2) estimate dFNC; (3) perform clustering state analysis; and (4) perform dynamic topologic analysis.

Group independent component analysis

We parcelled the fMRI data using a standard procedure of spatial GICA with the GIFT toolbox (mialab.mrn.org/software/gift/). First, we applied principal component analysis on the participant-specific data to reduce the data into 120 principal components,[16] which preserved more than 99% of the variance. Next, we concatenated the reduced data of all participants across time and further reduced the data to 100 principal components using an expectation maximization algorithm.[16] After estimating the group spatial maps, we applied a spatially constrained approach called group information-guided ICA[17] to perform back reconstruction of participant-specific spatial maps and corresponding time courses.

We identified as ICNs several independent components that had peak activation on gray matter, showed overlap with known brain regions, and exhibited primarily low frequency power. Compared to defining regions of interest based on anatomical brain atlases, ICNs identified by group ICA are functionally homogeneous and may be better at capturing individual differences of real functional boundaries in the brain.[15] We performed additional postprocessing steps on the time courses of selected ICNs, including (1) detrending linear, quadratic, and cubic trends; (2) conducting multiple regressions of the 6 realignment parameters and their temporal derivatives; (3) despiking detected outliers; and (4) low-pass filtering with a cutoff frequency of 0.15 Hz. After obtaining the spatial maps and time courses of all participants and completing the postprocessing steps described above, we calculated one-sample t test maps for each spatial map across participants and computed the mean power spectra of the corresponding time course for each ICN.

dFNC estimation

For each participant, we estimated dFNC between the time courses (170 time points) of ICNs using a sliding window approach. We used a tapered window, which was obtained by convolving a rectangle (window size = 20 × TR 40 seconds) with a Gaussian ($\sigma = 3$) to localize the dataset at each time point. The window was slid in steps of 1 TR, resulting in $T = 150$ total windows. The window size was selected based on the fMRI TR and according to previous studies showing that a window size in the range of 30 seconds–1 minute is a reasonable choice for capturing dynamic patterns in FC.[5,6,18] In addition, we verified the optimality of the selected window and reliability of findings by testing other window sizes. We determined that the results were similar among a wide range of window sizes (16–24 TR: 32–48 seconds). The results of other window sizes are provided in figures e-1 and e-2 (doi.org/10.5061/dryad.p1n53q4). We calculated the covariance matrix with windowed data to measure the dFNC between ICNs. The dFNC estimates of all windows for each participant were concatenated to form a $C \times C \times T$ array (where C denotes the number of ICNs and T denotes the number of windows), which represents the changes in FC between ICNs as a function of time.

State clustering analysis

To assess the dFNC patterns that reoccur over time, we conducted hard clustering on the dFNC estimates. We used the K-means clustering method with L1 distance function to cluster the windowed dFNC estimates into a set of separate clusters. Similar to EEG microstate analysis,[19] we first chose participant-specific exemplars, which are the time windows with local maxima in FNC variance across all connectivity pairs. Then, we conducted k-means clustering on these exemplars of all patients and controls combined and repeated it 100 times (with random initialization of centroid position) to obtain the group cluster centroids (functional dFNC states). The optimal number of centroid states was estimated by the elbow criterion, which is defined as the ratio of within-cluster distance to between-cluster distance. The optimal number of clusters was determined as $k = 5$, with each cluster representing a functional dFNC state. We also conducted k-means analysis using a different number of clusters ($k = 4, 6$) for comparison. These results are presented in figures e-3 and e-4 (doi.org/10.5061/dryad.p1n53q4). We used the obtained group centroids as the initial centroids to cluster each participant's windowed dFNC.

Next, we investigated whether MIG and HC presented different occurrences of different functional dFNC states during the course of the resting-state fMRI. We calculated the percentage occurrence of each dFNC state by dividing the number of time windows that were assigned to each state by the number of total windows. To count the occurrence of one state, we only used participant data with at least one window belonging to that state. We performed a 2-sample t test (control covariates: age and sex) to examine the group difference in occurrence between MIG and HC for each dFNC state.

We further investigated the presence of abnormal transient dFNC by examining the group difference in dFNC at each functional state. We performed a 2-sample t test (control covariates: age and sex) on each dFNC of each functional state to determine if there were dFNC changes in MIG. We then calculated the partial correlation between the abnormal dFNC and migraine pain frequency and intensity (control covariates: age, sex, SAS, and SDS) to explore the potential relationship between transient dFNC and migraine clinical symptoms. For correction of the multiple comparisons, all statistical results were corrected by false discovery rate (FDR) with a corrected significance level of $p < 0.05$.

Dynamic topologic analysis

We applied graph theory analysis to investigate the topologic organization of the functional dFNC states and compare it between MIG and HC. As discussed in the Results, we identified 52 ICNs. For this analysis, we defined those 52 ICNs as nodes and the dFNC between them as edges,[20] and we constructed a 52 × 52 connectivity matrix for each participant and each state. The graph theory analysis was performed using GRETNA software (nitrc.org/projects/gretna).[21] Similar to previous studies,[21,22] we first applied

a sparsity threshold S (the ratio of the number of actual edges to the maximum possible number of edges in a network) to sparsify all connectivity matrices that ranged from 0.1 to 0.35 with a step of 0.05 based on the ranges of previous studies.[23–25] We then generated an undirected and unweighted adjacency matrix for each participant and each state by setting edges as 1 or 0 (edges were designated as 1 if an edge between node i and node j was larger than the threshold we selected, and 0 if it was smaller than the threshold; absolute values of connectivity were considered).

For the adjacency matrix at each sparsity threshold, we calculated global and local network efficiency to investigate global and local information transfer.[20] In brief, we defined efficiency as inversely proportional to the harmonic mean of the shortest distance (number of edges) between all possible pairs of nodes. The global efficiency was the average efficiency across all node pairs, while the local efficiency was the average of the nodal local efficiency within neighbors of the node. To avoid the specific selection of a threshold, we applied an area under the curve (AUC) approach, which has been widely used in previous studies.[23,24] For each topologic measure, we calculated the AUC within the sparsity range and compared the AUC between MIG and HC for each dynamic state. We applied a 2-way analysis of variance with group (MIG vs HC) and state as factors to assess the differences of global and local efficiency. When the main effect was significant, we performed a post hoc 2-sample t test.

Data availability

All data in this study will be available upon reasonable request after publication. All in-house MATLAB codes can be requested from the authors.

Results

Clinical scores for migraine patients

Of the 100 patients, 9 were excluded due to incomplete scans (lack of resting-state fMRI scan or T1 anatomical scan), and 2 patients were excluded due to excessive head movement (>3 mm). Eighty-nine MIG and 70 HC were included in the study. A 2-sample t test and χ^2 test showed no significant difference of age and sex between the 2 cohorts ($p = 0.50$ and $p = 0.95$ for age and sex, respectively). We recorded behavioral scores for 87 patients (2 patients did not have a migraine diary). MIG had a headache frequency of 5.6 ± 3.3 and intensity of 5.6 ± 1.1 during the last month before the MRI scan. They had mild to moderate anxiety levels (SAS 45.0 ± 9.2) and were mildly depressed (SDS 45.3 ± 10.5), but the average scores were very close to the normal range (<45 for SAS and SDS). Other clinical symptoms, including photophobia, phonophobia, vomiting, and nausea, can be found in the table.

Intrinsic connectivity networks

The 52 identified ICNs were categorized into 6 functional domains that have been widely studied in migraineurs[26]

Table Demographics and clinical characteristics of migraine without aura patients (MIG) and healthy controls (HC)

	MIG	HC
N	89	70
Age, y	22.0 ± 2.3	22.2 ± 1.0
Sex, M	22	18
Duration, mo	68.0 ± 34.7	NA
Headache frequency	5.6 ± 3.3	NA
Headache duration, h	8.0 ± 9.6	NA
Headache intensity (VAS)	5.6 ± 1.1	NA
Light sensitivity	50/87	NA
Sound sensitivity	59/87	NA
Vomiting	13/87	NA
Nausea	45/87	NA

Abbreviations: NA = not applicable; VAS = visual analogue scale.
Values are mean ± SD or n/N.

(figure 2): subcortical domain (SC), auditory domain (AUD), visual domain (VS), sensorimotor domain (SM), cognitive control domain (CC), and default mode domain (DM).

Interestingly, we identified 2 ICNs for the thalamic nuclei in the SC. Given the group difference of state occurrences and state-based transient dFNC patterns that are described below, we further examined these functional ICNs to determine their anatomical location in the thalamus using the MNI atlas and the BrainNavigator atlas (thehumanbrain.net/navigator). We found that these 2 ICNs included the medial thalamus and posterior thalamus (figure 2, bottom panel). Previous studies using human and rat models have suggested that the posterior thalamus sends broad projections to several cortical areas and might be a distinct feature of migraine pathology.[27] The detailed component labels and peak coordinates of each ICN are provided in table e-1 and figures e-5–e-11 (doi.org/10.5061/dryad.p1n53q4).

Group difference of occurrences and dFNC patterns

The cluster centroid of each dFNC state and the group difference in occurrences (time spent in each state) are presented in figure 3. MIG had a significantly higher occurrence rate in state 1 ($p = 0.00009$, $p_{FDR} < 0.05$) and a significantly lower occurrence rate in state 2 ($p < 0.00001$, $p_{FDR} < 0.05$). As shown in figure 3B, dFNC patterns are different among the identified states. In state 1, we observed strong positive connectivity within the SM and VS, negative connectivity between the SC and VS, SM, and AUD, and negative connectivity between the DM and AUD, SM, and VS. We found strong positive connectivity within the VS in all 5 states.

Figure 2 Spatial maps of the 52 identified intrinsic connectivity networks (ICNs) sorted into 6 resting-state domains
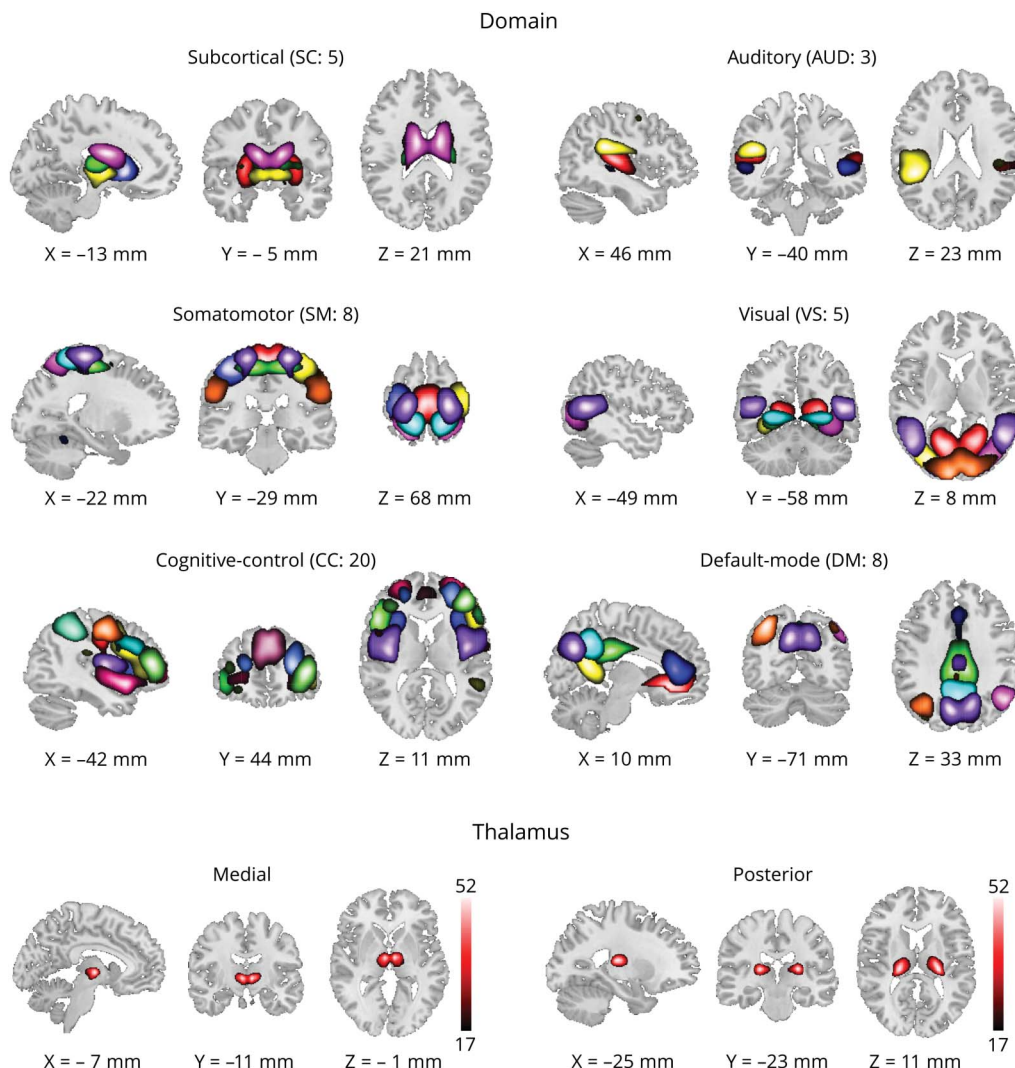
Two thalamic nuclei were identified. Each color in the spatial maps corresponds to a different ICN.

State 2 was sparsely connected, but we observed strong positive connectivity within the DM.

Within each state, MIG exhibited abnormal transient dFNC patterns compared to HC (figure 3, C and D). In state 1, MIG had lower connectivity between the SC and VS as well as between the VS and DM. However, there was higher connectivity between the VS and SM. In other states, MIG had stronger connectivity between the VS and SM, but decreased connectivity within the VS. In addition, we also observed weaker connectivity between the VS and CC in state 2, state 3, and state 5. It should be noted that abnormal FC of migraineurs in these 6 networks has been reported and reviewed in previous studies,[26] but findings have not been not consistent. In figure 3D, we show how abnormal connectivity in these networks is transient. This may be a reason for the inconsistent findings in previous studies.

Since many migraneurs had photophobia (n = 50) and phonophobia (n = 59), we performed an exploratory analysis comparing occurrence rates between patients with and without photophobia (or phonophobia), and we did not find any difference between patients with and without those symptoms. The detailed results can be found in figures e-12 and e-13 (doi.org/10.5061/dryad.p1n53q4).

Association of thalamocortical dFNC and migraine symptoms

Considering the significantly higher occurrence of MIG in state 1, abnormal dFNC of subcortical structures such as the medial and posterior thalami and dorsal striatum (putamen and caudate) with other networks, and thalamocortical pathophysiology in migraine, we were particularly interested in disrupted dFNC between the medial/posterior thalami and other cortical regions in state 1 (as shown by the red rectangular box in the connectivity matrix of
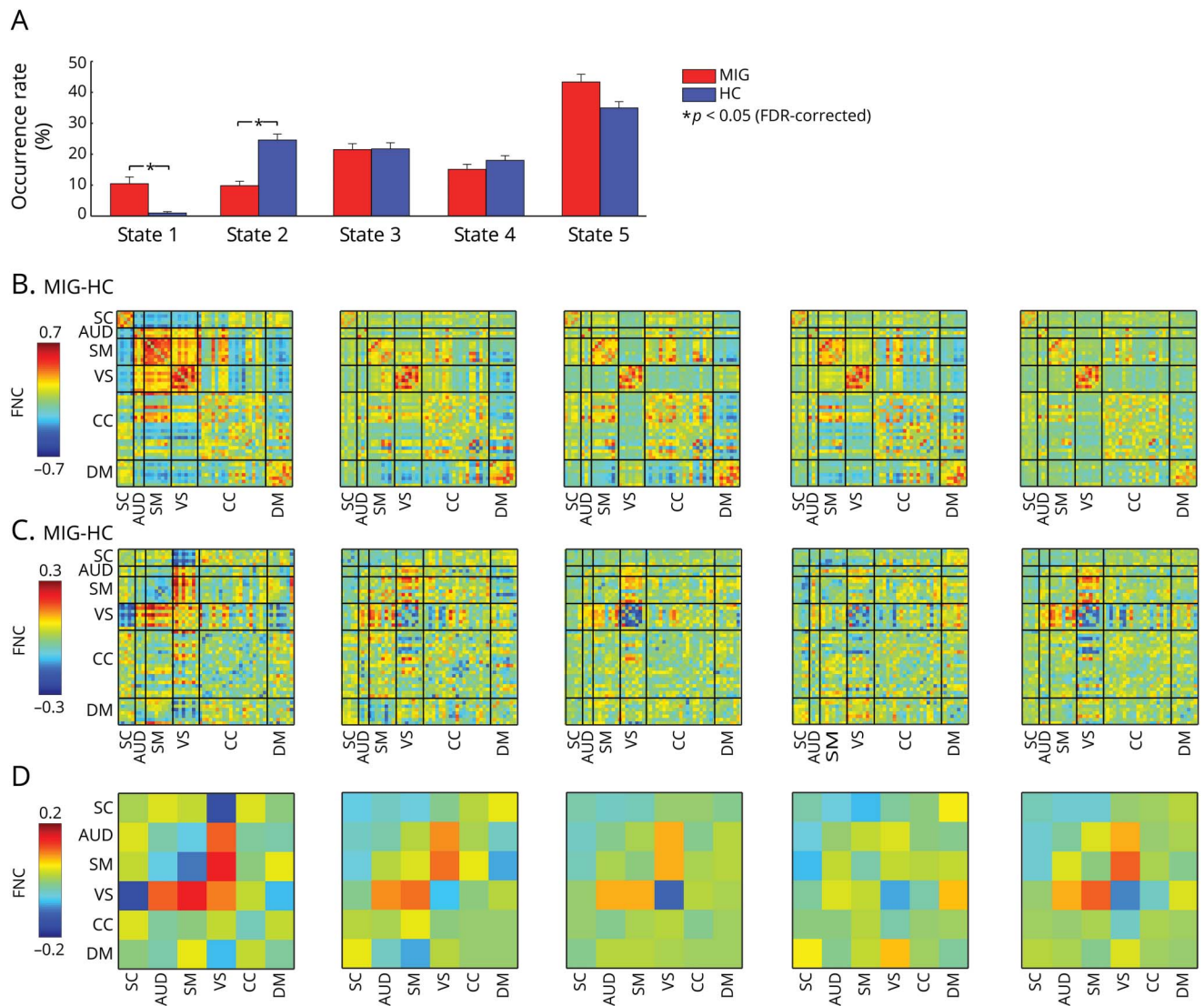
(A) Group difference in percentage of occurrences of 5 dFNC states. Bar represents the mean occurrence of each state, while error bar represents the standard error of mean of occurrence. Two out of 5 states have significant group difference. Asterisks indicate the significance (false discovery rate [FDR]–corrected, $p < 0.05$). (B) Cluster centroids of the 5 dFNC states. (C) Group difference of dFNC of 52 brain regions between migraine without aura patients (MIG) and healthy controls (HC) in the 5 states. (D) Group difference of dFNC of 6 selected brain networks between MIG and HC in 5 states. AUD = auditory domain; CC = cognitive control domain; DM = default mode domain; SC = subcortical; SM = sensorimotor domain; VS = visual domain.

figure 4) as well as its associations with migraine symptoms. Our analyses showed that in state 1, the more strongly negative transient dFNC between the posterior thalamus and middle occipital gyrus was significantly correlated with headache frequency ($r = -0.49$, $p = 0.006$, $p_{FDR} < 0.05$), and the more strongly positive transient dFNC between the posterior thalamus and precuneus was also significantly associated with headache frequency ($r = 0.48$, $p = 0.0006$, $p_{FDR} < 0.05$). We replicated these results using different lengths of sliding windows and clusters (figures e-1–e-3, doi.org/10.5061/dryad.p1n53q4). We did not find any significant associations between the medial thalamus and clinical symptoms. We also performed exploratory analyses by checking the associations between all dFNC pairs

and clinical symptoms in every state, and no associations passed statistical thresholding.

Dynamic network efficiency

We calculated topologic measures of functional dFNC states per participant and compared them between groups. Figure 5 shows the mean and smoothed density histograms for global and local efficiencies for each group and each dFNC state. In general, patients with migraine had lower global efficiency ($F_{1,149} = 16.0$, $p < 0.001$) and local efficiency ($F_{1,149} = 11.8$, $p < 0.001$), suggesting that parallel information transfer in the global and local functional networks was less efficient in migraineurs. We also observed significant effects of temporal dynamics

Figure 4 Abnormal transient thalamus dynamic functional network connectivity (dFNC) and its association with migraine symptoms
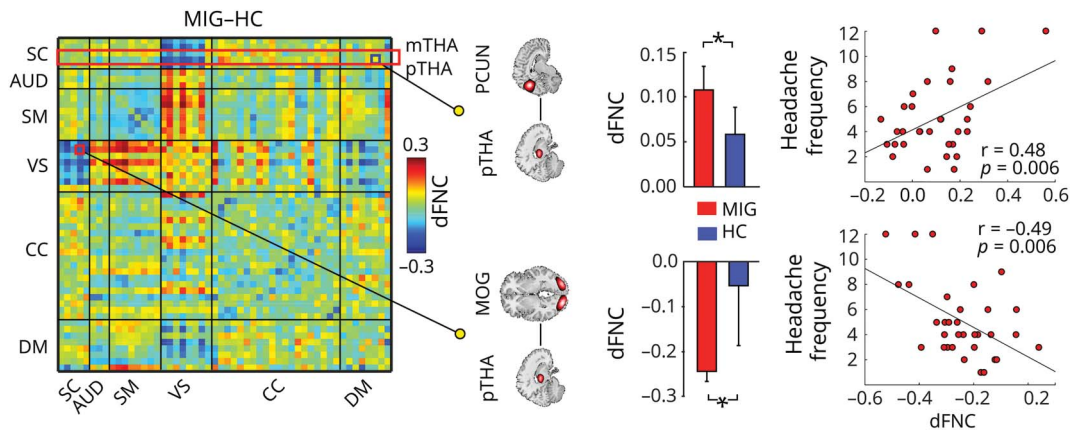
In state 1, migraine patients had significantly stronger positive dFNC between the posterior thalamus (pTHA) and precuneus (PCUN) and stronger negative dFNC between the pTHA and middle occipital gyrus (MOG). The strength of dFNC was associated with headache frequency of migraine patients. The red rectangular box in the connectivity matrix highlights thalamus (medial and posterior) connectivity. Asterisks indicate significance (false discovery rate corrected, $p < 0.05$). AUD = auditory domain; CC = cognitive control domain; DM = default mode domain; HC = healthy controls; MIG = migraine without aura patients; mTHA = medial thalamus; SC = subcortical; SM = sensorimotor domain; VS = visual domain.

(across 5 states) on global efficiency ($F_{4,149} = 40.1$, $p < 0.001$) and local efficiency ($F_{4,149} = 36.4$, $p < 0.001$),

Figure 5 Topologic measures in dynamic functional connectivity
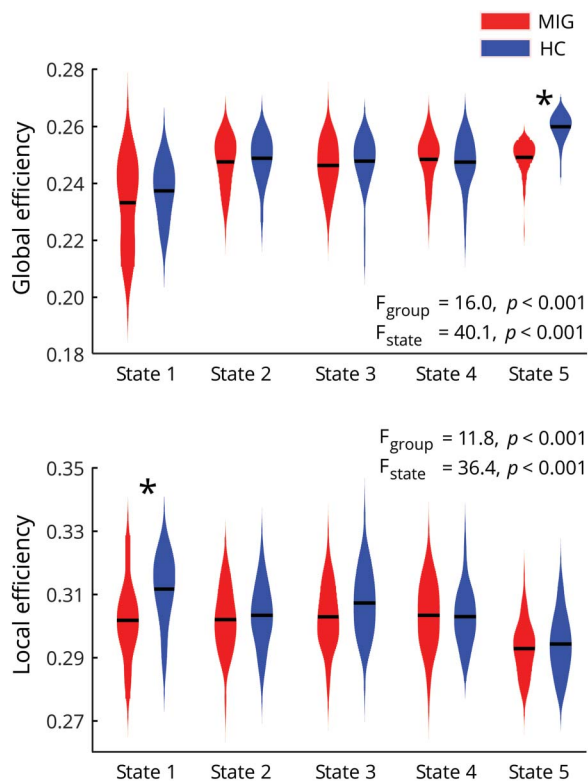
The global and local efficiencies in different dynamic states are shown using violin plots for the migraine patients (red) and healthy controls (blue). Horizontal lines indicate group means (black). Asterisks represent significant difference at $p_{FDR} < 0.05$. HC = healthy controls; MIG = migraine without aura patients.

indicating that functional networks exhibited variable efficiency of information transfer in the time-varying brain connectivity. Post hoc comparisons showed that migraine patients had lower global efficiency in state 5 ($p < 0.001$, $p_{FDR} < 0.05$) and lower local efficiency in state 1 ($p = 0.003$, $p_{FDR} < 0.05$).

Discussion

Given the known dynamic, condition-dependent nature of brain activity, it is natural to expect that FC will exhibit variation over time.[5] In a recent article,[28] the authors used simultaneous calcium and intrinsic signal imaging on mice. They found evidence of the neuronal origin of dynamic FC and suggested that information relevant to FC is condensed in temporally sparse events. In another study, Ma and Zhang[29] found that temporal organization of dynamic FC patterns followed specific sequential orders in awake rates and humans. In the present study, we identified 5 reoccurring dFNC states that exhibited significantly different connectivity patterns. Negative dFNC between subcortical regions and sensory, visual regions was only observed in state 1. Visual regions were highly synchronous in every state, but their connectivity strength was different (state 1 had the strongest visual synchronization). State 2 was sparsely connected, but with strong positive connectivity within default mode regions. This might be indicative of a lower attentional state. State 5, which had weak dFNC patterns that resembled static FNC patterns, was the most frequently reoccurring state in both groups. These observations were consistent with previous findings on dFNC states.[6,18]
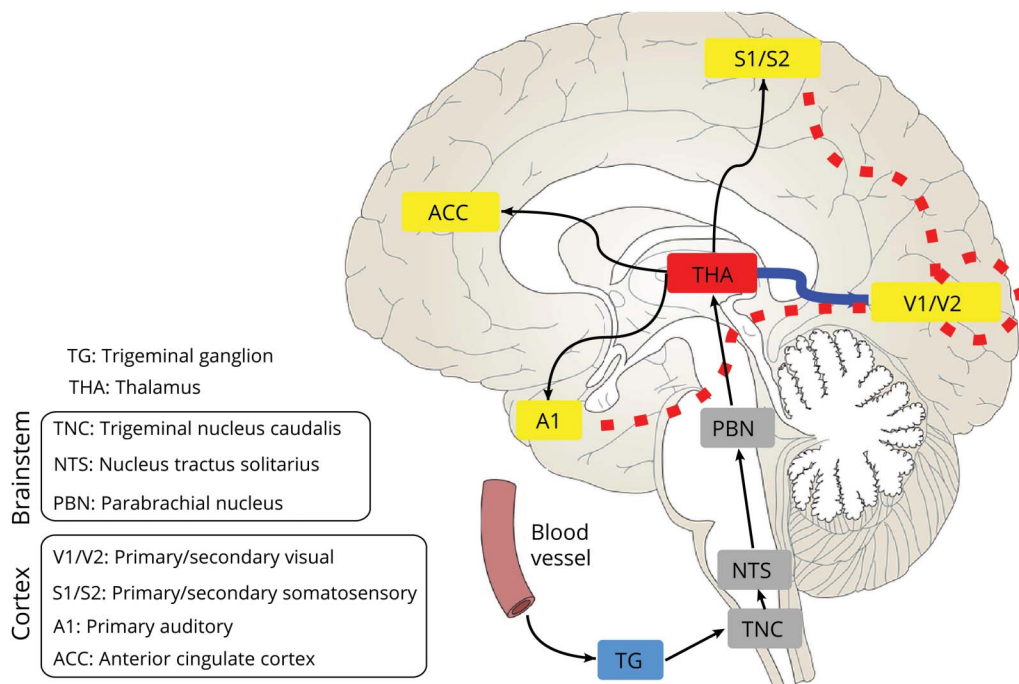
Clinical populations, such as patients with schizophrenia and bipolar disorder,[30] major depression,[7] Parkinson disease,[23] autism,[31] or Alzheimer disease,[32] experience significant changes in dynamic properties. In this study, we found that migraine patients had significantly different occurrences in 2 different states. Migraineurs spent more time in state 1, which was characterized by strong negative dFNC between subcortical and cortical regions. We hypothesize that the increased occurrence of state 1 for migraineurs may be due to the abnormal cortical–subcortical interaction in migraine patients.[33] More specifically, it may stem from abnormalities in the thalamocortico-thalamic network. In addition, our analysis pipeline, in a completely data-driven approach, specifically delineated the posterior–pulvinar thalamic complex as a functional component that differentiated migraineurs from healthy controls. The pulvinar nucleus in this region sends broad projections to the V1, V2, auditory, and somatosensory cortices (figure 6), and these projections are implicated in clinical features of migraine.[27] This region is mostly a higher-order relay, and its projections facilitate its involvement in integrating multisensory information as well as transmitting information from higher layers of one cortical area to another.[34] These functions may further associate this region with the multisensory information processing dysfunction in migraineurs, even interictally.[35]

Previous studies have shown that abnormalities in internally generated low-frequency oscillations in the thalamocortical network can disrupt and interfere with the flow of information between the thalamus and cortex with consequent disturbances in sensory, cognitive, and motor neural processes in migraineurs.[1,2,36] Recent studies that investigated abnormal thalamocortical network activity using structural and functional MRI have also supported our findings.[37,38] Researchers found abnormal interaction between the thalamus and visual processing areas in migraineurs between attacks that in turn could lead to disrupted activation of the default mode network. Such associations between the thalamus and visual/default mode network were directly revealed by our study. Furthermore, abnormalities in thalamocortico-thalamic connectivity may disrupt habituation to external stimuli. Indeed, lack of habituation is a well-characterized aspect of migraine disease that may also account for hyperexcitability in migraineurs. Such hyperexcitability may be caused by abnormalities in thalamocortico-thalamic connectivity and lead to thalamocortical dysrhythmia (TCD).

Migraine patients spent more time in state 1 and less time in state 2, which had stronger default mode connectivity. This suggests that patients may spend less time in a wandering mental state, which is associated with weaker alpha band oscillation.[39] This aligns with TCD of migraine pathophysiology, which suggests that normal resting-state alpha activity slows down to theta frequency (alpha reduced), and theta activity is associated with an increase in beta/gamma activity. The lower occurrence of migraine patients in state 2 might

Figure 6 Migraine-relevant multisensory networks

TG: Trigeminal ganglion
THA: Thalamus

Brainstem
TNC: Trigeminal nucleus caudalis
NTS: Nucleus tractus solitarius
PBN: Parabrachial nucleus

Cortex
V1/V2: Primary/secondary visual
S1/S2: Primary/secondary somatosensory
A1: Primary auditory
ACC: Anterior cingulate cortex

The posterior nucleus of the thalamus (pTHA) receives projections from the brainstem and relays to the primary and secondary somatosensory cortices (S1 and S2), insula (not shown in the figure), primary and secondary visual cortices (V1/V2), primary auditory cortex (A1), and anterior cingulate cortex (ACC). A detailed review of migraine-relevant networks can be found in reference 27. We found abnormal connections between the pTHA and visual cortex (blue line) and hyperconnectivity (red dashed lines) between the sensory cortices (visual, somatosensory, and auditory) in the migraine pathologic state.

stem from reduced alpha activity, possibly making it more difficult to enter a wandering mental state. In other words, our results suggest that reduced duration of high alpha activity can lead to reduced overall alpha activity in migraineurs.

Aside from atypical thalamocortical networks, we also found abnormal dFNC within the VS, as well as between the VS and other networks, in migraineurs (figure 6). This may suggest that the hyperexcitability of the visual cortex may be linked to altered dFNC (stronger negative connectivity of the VS with the DM and SC, and positive connectivity between the VS and SM). This finding is consistent with existing literature on the pathophysiologic basis of migraine. For instance, the visual cortex is hyperexcitable in interictal migraine for both migraine with and without aura.[40,41] Further exploratory analyses demonstrated that migraineurs with and without photophobia did not differ in occurrence rates of dFNC states. Since the patients in our study were in the interictal stage, this finding may further support the specificity of these abnormal dFNCs to the brain's functional architecture in migraine. We also speculate that during or around an attack, these dFNCs may no longer be functioning similarly, and there may be differences between those with and without photophobia. In addition, although most patients in our study reported that they had phonophobia during the month before the MRI scan, we did not find any abnormal auditory dFNC or any difference between occurrence rates between those with and without phonophobia. These results are consistent with previous studies reporting that interictal migraineurs do not show abnormal functional and structural brain activity and connectivity in the auditory cortices.[26,40,42,43]

Previous studies have suggested that global dysfunction in multisensory information processing and integration characterizes migraineurs in the interictal period.[44] In our study, we applied topologic measures to examine the global and local efficiencies of information transfer in migraine patients, thus providing direct evidence of disrupted functional segregation and integration in brain networks of migraine patients.

There are several limitations to this study. First, we speculated that the abnormal dFNC in thalamocortical networks might be associated with thalamocortical dysrhythmia and lead to dysfunction of multisensory integration. However, it is unclear how these abnormalities in dFNC influence sensory processing during stimulation. Our hypothesis could be further corroborated by conducting dFNC state analysis on a task fMRI dataset that specifically probes the sensory (e.g., somatosensory, visual) processes. Second, migraine patients might have different levels of vigilance compared to HC, and dFNC could be modulated by the fluctuating vigilance during MRI scans. Unlike other artifacts (e.g., noise, head motion), FC changes related to changes in vigilance are physiologically meaningful. We have also examined the level of vigilance between the 2 groups of participants using well-established rsFC signatures of vigilance,[45] and results showed no systematic differences between MIG and HC (appendix e-3, doi.org/10.5061/dryad.p1n53q4). Future studies should include cardiac, respiratory, or eye-tracking data[46] to further characterize the pathophysiology of migraine patients.

In the present study, we found dynamic properties of abnormal thalamocortical networks coupled with clinical symptoms as well as disrupted functional segregation and integration of dynamic FC in migraine patients. These results extend current findings regarding thalamocortical dysrhythmia in the migraine brain and suggest migraine-related deficits of brain functions in the interictal state.

Appendix Authors

Name	Location	Role	Contribution
Yiheng Tu, PhD	Massachusetts General Hospital, Charlestown	Author	Designed and conceptualized study, analyzed the data, drafted the manuscript for intellectual content
Zening Fu, PhD	The Mind Research Network, Albuquerque, NM	Author	Analyzed the data, revised the manuscript for intellectual content
Fang Zeng, MD, PhD	Chengdu University of Traditional Chinese Medicine, Sichuan, China	Author	Major role in the acquisition of data
Nasim Maleki, PhD	Massachusetts General Hospital, Charlestown	Author	Interpreted the data, revised the manuscript for intellectual content
Lei Lan, MD, PhD	Chengdu University of Traditional Chinese Medicine, Sichuan, China	Author	Major role in the acquisition of data, revised the manuscript for intellectual content

Continued

References

1. Llinás RR, Ribary U, Jeanmonod D, Kronberg E, Mitra PP. Thalamocortical dysrhythmia: a neurological and neuropsychiatric syndrome characterized by magnetoencephalography. Proc Natl Acad Sci USA 1999;96:15222–15227.
2. Hodkinson DJ, Wilcox SL, Veggeberg R, et al. Increased amplitude of thalamocortical low-frequency oscillations in patients with migraine. J Neurosci 2016;36:8026–8036.
3. Delamillieure P, Doucet G, Mazoyer B, et al. The resting state questionnaire: an introspective questionnaire for evaluation of inner experience during the conscious resting state. Brain Res Bull 2010;81:565–573.
4. Kucyi A, Davis KD. Dynamic functional connectivity of the default mode network tracks daydreaming. Neuroimage 2014;100:471–480.
5. Hutchison RM, Womelsdorf T, Allen EA, et al. Dynamic functional connectivity: promise, issues, and interpretations. Neuroimage 2013;80:360–378.
6. Damaraju E, Allen EA, Belger A, et al. Dynamic functional connectivity analysis reveals transient states of dysconnectivity in schizophrenia. Neuroimage Clin 2014;5:298–308.
7. Demirtas M, Tornador C, Falcon C, et al. Dynamic functional connectivity reveals altered variability in functional connectivity among patients with major depressive disorder. Hum Brain Mapp 2016;37:2918–2930.
8. Marusak HA, Calhoun VD, Brown S, et al. Dynamic functional connectivity of neurocognitive networks in children. Hum Brain Mapp 2016;108:97–108.
9. Headache Classification Subcommittee of the International Headache Society. The International Classification of Headache Disorders: 2nd edition. Cephalalgia 2004;24(suppl 1):9–160.
10. Ashburner J, Friston KJ. Unified segmentation. Neuroimage 2005;26:839–851.
11. Ciric R, Wolf DH, Power JD, et al. Benchmarking of participant-level confound regression strategies for the control of motion artifact in studies of functional connectivity. Neuroimage 2017;154:174–187.
12. Tfelt-Hansen P, Block G, Dahlöf C, et al. Guidelines for controlled trials of drugs in migraine: second edition. Cephalalgia 2000;20:765–786.
13. Zung WWK. A rating instrument for anxiety disorders. Psychosomatics 1971;12:371–379.
14. Zung WWK. A self-rating depression scale. Arch Gen Psychiatry 1965;12:63–70.
15. Calhoun VD, Adali T, Pearlson GD, Pekar JJ. A method for making group inferences from functional MRI data using independent component analysis. Hum Brain Mapp 2001;14:140–151.
16. Erhardt EB, Rachakonda S, Bedrick EJ, Allen EA, Adali T, Calhoun VD. Comparison of multi-subject ICA methods for analysis of fMRI data. Hum Brain Mapp 2011;32:2075–2095.
17. Du Y, Fan Y. Group information guided ICA for fMRI data analysis. Neuroimage 2013;69:157–197.
18. Allen EA, Damaraju E, Plis SM, Erhardt EB, Eichele T, Calhoun VD. Tracking whole-brain connectivity dynamics in the resting state. Cereb Cortex 2014;24:663–676.
19. Van de Ville D, Britz J, Michel CM. EEG microstate sequences in healthy humans at rest reveal scale-free dynamics. Proc Natl Acad Sci USA 2010;107:18179–18184.
20. Rubinov M, Sporns O. Complex network measures of brain connectivity: uses and interpretations. Neuroimage 2010;52:1059–1069.
21. Wang J, Wang X, Xia M, Liao X, Evans A, He Y. GRETNA: a graph theoretical network analysis toolbox for imaging connectomics. Front Hum Neurosci 2015;9:386.
22. Keown CL, Datko MC, Chen CP, Maximo JO, Jahedi A, Müller RA. Network organization is globally atypical in autism: a graph theory study of intrinsic functional connectivity. Biol Psychiatry Cogn Neurosci Neuroimaging 2017;2:66–75.
23. Kim J, Criaud M, Cho SS, et al. Abnormal intrinsic brain functional network dynamics in Parkinson's disease. Brain 2017;140:2955–2967.
24. Zhang J, Wang J, Wu Q, et al. Disrupted brain connectivity networks in drug-naive, first-episode major depressive disorder. Biol Psychiatry 2011;70:334–342.
25. Hashmi JA, Loggia ML, Khan S, et al. Dexmedetomidine disrupts the local and global efficiencies of large-scale brain networks. Anesthesiology 2017;126:419–430.
26. Maleki N, Gollub RL. What have we learned from brain functional connectivity studies in migraine headache? Headache 2016;56:453–461.
27. Brennan KC, Pietrobon D. A systems neuroscience approach to migraine. Neuron 2018;97:1004–1021.
28. Matsui T, Murakami T, Ohki K. Neuronal origin of the temporal dynamics of spontaneous BOLD activity correlation. Cereb Cortex 2019;129:1496–1508.
29. Ma Z, Zhang N. Temporal transitions of spontaneous brain activity in awake rats. eLife 2018;7:e33562.
30. Fu Z, Tu Y, Di X, et al. Characterizing dynamic amplitude of low-frequency fluctuation and its relationship with dynamic functional connectivity: an application to schizophrenia. Neuroimage 2018;180:619–631.
31. Fu Z, Tu Y, Di X, et al. Transient increased thalamic-sensory connectivity and decreased whole-brain dynamism in autism. Neuroimage Epub 2018 Jun 6.
32. Jones DT, Vemuri P, Murphy MC, et al. Non-stationarity in the "resting brain's" modular architecture. PLoS One 2012;7:e39731.
33. Hubbard CS, Khan SA, Keaser ML, Mathur VA, Goyal M, Seminowicz DA. Altered brain structure and function correlate with disease severity and pain catastrophizing in migraine patients. eNeuro 2014;1:e20.14.
34. Sherman SM. The thalamus is more than just a relay. Curr Opin Neurobiol 2007;17:417–422.
35. Schwedt TJ. Multisensory integration in migraine. Curr Opin Neurol 2013;26:248–253.
36. Coppola G, Bracaglia M, Di Lenola D, et al. Lateral inhibition in the somatosensory cortex during and between migraine without aura attacks: correlations with thalamocortical activity and clinical features. Cephalalgia 2016;36:568–578.
37. Coppola G, Di Renzo A, Tinelli E, et al. Thalamo-cortical network activity between migraine attacks: insights from MRI-based microstructural and functional resting-state network correlation analysis. J Headache Pain 2016;17:100.
38. Amin FM, Hougaard A, Magon S, et al. Altered thalamic connectivity during spontaneous attacks of migraine without aura: a resting-state fMRI study. Cephalalgia 2018;38:1237–1244.
39. Kucyi A, Salomons TV, Davis KD. Mind wandering away from pain dynamically engages antinociceptive and default mode brain networks. Proc Natl Acad Sci USA 2013;110:18692–18697.
40. Mulleners WM, Chronicle EP, Palmer JE, Koehler PJ, Vredeveld JW. Visual cortex excitability in migraine with and without aura. Headache 2001;41:565–572.
41. Aurora S, Cao Y, Bowyer S, Welch KMA. The occipital cortex is hyperexcitable in migraine: experimental evidence. Headache 1999;39:469–476.
42. Pietrobon D, Moskowitz MA. Pathophysiology of migraine. Annu Rev Physiol 2013;75:365–391.
43. Ashkenazi A, Mushtaq A, Yang I, Oshinsky M. Ictal and interictal phonophobia in migraine: a quantitative controlled study. Cephalalgia 2009;29:1042–1048.
44. Schwedt TJ, Schlaggar BL, Mar S, et al. Atypical resting-state functional connectivity of affective pain regions in chronic migraine. Headache 2013;53:737–751.
45. Tagliazucchi E, von Wegner F, Morzelewski A, Borisov S, Jahnke K, Laufs H. Automatic sleep staging using fMRI functional connectivity data. Neuroimage 2012;63:63–72.
46. Allen EA, Damaraju E, Eichele T, Wu L, Calhoun VD. EEG signatures of dynamic functional network connectivity states. Brain Topogr 2018;31:101–116.